Permeation of *N*-Butane, Propane and Ethane Through Ethylcellulose

ERTUGRUL CASUR and THEODORE G. SMITH,* *Department of Chemical Engineering, University of Maryland, College Park, Maryland 20742*

Synopsis

The permeation of *n*-butane, propane, and ethane in ethylcellulose has been measured over a pressure range from 25 to 200 mm Hg and over the temperature range from 30 to 70°C. The permeation and diffusional time lag of each of the three gases in ethylcellulose is pressure dependent. Transport of the gases through ethylcellulose can be described by the partial immobilization model. It was found that, in general, the Langmuir-mode species diffusion coefficients are lower than the Henry's law species diffusion coefficients. The logarithm of diffusion coefficients at zero penetrant concentration varies linearly with the square of the molecular diameter of *n*-butane, propane, and ethane permeating through ethylcellulose. This relationship suggests that the diffusion process depends upon the availability of sufficient cross-sectional area for the penetrant to diffuse. An Arrhenius temperature dependence was observed for permeation coefficients and diffusion coefficients for *n*-butane, propane, and ethane in ethylcellulose. The activation energy of diffusion at zero penetrant concentration is directly proportional to the square of the gas molecular diameter and the entropy of activation. This observation is consistent with the view that the activation energy of diffusion is associated with the energy required to produce a space of sufficient cross-section for the diffusion molecule to pass.

INTRODUCTION

It has been shown that sorption in this system can be considered to be dominated by two mechanisms.[1] One mechanism is ordinary dissolution described by Henry's law, and the second mechanism is sorption in microvoids in the polymer structure, described by the Langmuir isotherm. This description of sorption is known as the dual sorption theory.[3] This can be represented mathematically as

$$C = C_D + C_H \tag{1}$$

$$C = k_D p + \frac{C_H' bp}{1 + bp} \tag{2}$$

where c is the total concentration of sorbed penetrant, C_D is the sorption of the species following Henry's law, C_H is the sorption in microvoids following the Langmuir isotherm, k_D is the Henry's law constant, C_H' is the microvoid saturation constant, b is the microvoid affinity constant, and p is the pressure.

* To whom correspondence should be addressed.

Journal of Applied Polymer Science, Vol. 31, 1441-1468 (1986)

CCC 0021-8995/86/051441-28 $04.00

Consider mass transfer in a situation in which one face of an initially degassed film is exposed to a penetrant gas while the other surface is kept at zero concentration (i.e., zero pressure). The gas dissolves at the high-pressure side of the film and diffuses through the film. The flux J is given by Fick's first law of diffusion:

$$J = -D \frac{\delta C}{\delta x} \tag{3}$$

Vieth and Sladek[4] have developed a technique for estimating diffusion rates from transient sorption data. They assumed that gas trapped in microvoids is immobilized and the driving force for diffusion is the concentration gradient of the dissolved species. Later studies of Vieth et al.[5,6] concerning the sorption of CO_2, CH_4, Ar, and N_2 in glassy polystyrene lent support to the validity of using this technique. The mathematical formulation of the dual sorption affect on the time lag and permeability has been developed by Paul.[7] The time lag expression

$$\theta = \frac{l^2}{6D}(1 + Kf(y)) \tag{4}$$

where $y = bp$

p = upstream pressure

$f(y) = 6y^{-3}(0.5y^2 + y - (1 + y)\ln(1 + y))$

was obtained from the application of an asymptotic steady-state solution to the dual sorption diffusion model developed by Vieth and Sladek and experimentally verified by Paul and Kemp.[8]

In the derivation of eq. (4), it was assumed that the penetrant molecules sorbed by the Langmuir isotherm mode are completely immobilized and do not contribute to the diffusive flux. Under these conditions, the permeability is independent of upstream pressure. As indicated by eq. (4), the time lag is strongly dependent on the upstream pressure. The conventional time lag expression $l^2/6D$ is increased by the factor of $(1 + kF(y))$ because of the time required to fill the microvoids. The Langmuir isotherm mode of sorption removes and immobilizes the penetrant molecules from the diffusive flux and thus increases the time required to reach steady state.

Petropoulos[9] has proposed the partial immobilization of gas molecules, sorbed by the Langmuir mode, and Paul and Koros[10] have formulated the effect of partially immobilizing sorption on permeability and time lag. They assigned different diffusion coefficients to the gas sorbed by each of the two sorption mechanisms. The expression describing the partial immobilization model permeability and diffusion time lag are a function of upstream gas pressure. The partial immobilization model has been applied to several systems.[11-13] It has been shown for the above systems that the diffusivity attributed to the Langmuir-mode species is much lower than the diffusivitity attributed to the Henry's law species.

The original assumptions of the dual sorption model have been stated by Vieth et al.[3] Later, some of these assumptions were relaxed by several investigators. The positive deviation from Henry's law is observed when

sorption of penetrant swells the polymer matrix. The swelling increases the number of Langmuirian sorption sites with concomitant increase in the sorption capability with the penetrant concentration.

EXPERIMENTAL

Materials

The ethylcellulose used in this study is the same standard Ethocel 10 cps made by the Dow Chemical Company used in our previously reported sorption study.[1] *n*-butane, propane, and ethane used in the sorption study were also used in this permeation study. Films were prepared by dissolving ethylcellulose in butyl acetate followed by casting on a mercury surface.

Permeation Experiment

The major component of the permeation experiment is the permeation cell. The permeation cell used in this study was designed and used by Yi.[14] The cell is made of brass, and a sample film to be evaluated is secured in place by metal clamping rings. To prevent the film from rupturing or sagging, the low-pressure side of the film is supported by a sintered metal disk. The remainder of the permeation apparatus is shown in Figure 1. It consists of a buffer volume and a mercury manometer upstream from the permeation cell; a calibrated volume and a thermocouple vacuum pressure measuring gage downstream of the permeation cell, and air bath temperature-regulating system. Since the thermal conductivity of a gas is dependent on the type of gas and the pressure, the thermocouple vacuum gage was calibrated with a McLeod gage for each gas, and calibration curves, pressure versus millivolts, were constructed. The downstream gas receiver volume below the membrane, including the pore volume of the sintered metal disk, was carefully measured by a liquid filling technique. Downstream volume was kept as large as possible in order to satisfy the boundary conditions of the mathematical model used in data analysis. Since a very small pressure increase is measured over a long period of time during the steady-state permeation experiment, careful attention was paid to the prevention of leaks into the downstream volume. After an extended period of degassing,

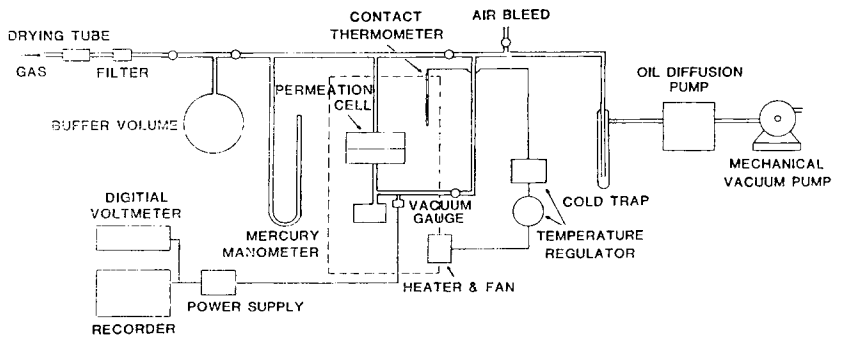

Fig. 1. Schematic diagram of pemeation apparatus.

the gas was introduced into the system and the pressure in the downstream volume was checked for leaks before each permeation experiment. A blank test was also performed to detect leaks into the downstream volume. Results from this experiment indicated that the downstream volume was leak proof since a pressure increase of only 2 μm Hg occurred over a 3-h period.

For each permeation experiment, the following procedure was followed.[2] After the average thickness of the film was determined, the film was sealed in the cell, the cell assembled, and a sufficient period was permitted to elapse so that the desired temperature could be obtained. A high vacuum was then applied to degas the film and the system. Degassing was continued until no pressure increase was observed in the portion downstream of the permeation cell when the valve between the downstream portion of the cell and the vacuum line was closed off. Samples were allowed to degas at least 48 h at a pressure of 3–5 μm Hg. At the end of the degassing period, the vacuum line was sealed and the desired amount of gas was introduced into the chamber connected to the upstream side of the film. The downstream side of the film was initially at nearly zero pressure (3–5 μm Hg). As the gas permeates through the film, pressure increases in the volume connected to the downstream side of the permeation cell. This pressure increase was measured with the thermocouple vacuum gage and the experiment continued until steady-state permeation was reached. The same procedure was repeated when the experimental temperature, gas, or the sample film was changed.

Estimation of the Transport Parameters

The steady-state permeation experiment allows the determination of the permeation coefficient and the diffusion time lag. The cumulative amount of penetrant Q_t can be calculated from the downstream pressure and volume. The plot of Q_t as a function of time is composed of a nonlinear transient portion and a linear steady-state portion. Permeation can be calculated from the slope of the steady-state portion of the plot by using the relation

$$P = V\left(\frac{\Delta P}{\Delta t}\right)_s \frac{273}{273 + T}\frac{1}{76}\frac{l}{A}\frac{1}{p} \tag{5}$$

where V is the downstream system volume in cm^3, T is the temperature in °C, l is the thickness of the film in cm, A is the area of the film in cm^2, p is the gas pressure at the upstream side of the film in cm Hg, and $(\Delta p/\Delta t)_s$ is the steady-state rate of increase in pressure in the system volume downstream of the film in cm Hg/s. Extrapolation of the steady-state portion of the time axis yields the time lag and diffusivity.

RESULTS AND DISCUSSION

Steady-State Permeability

The permeability of *n*-butane, propane, and ethane through ethylcellulose was measured in the pressure range of from nearly 0 to 20 cm Hg and over the temperature range of 30–70°C. Five upstream pressures—25, 50, 100,

150, and 200 mm Hg—were chosen to determine the permeability coefficients at 10°C increments. A typical permeation plot from which the permeability coefficients and the time lags were determined is shown in Figure 2.

Figures 3 through 5 show the permeability of *n*-butane, propane, and ethane, respectively, at several upstream pressures and temperatures. The permeability coefficients are tabulated in Table I. The data in the literature for *n*-butane, propane, and ethane permeation through ethylcellulose available for comparison is that given by Hsieh.[15] The reported permeabilities at 25°C are as follows: *n*-butane at 45.1 mm Hg pressure, 3.87×10^{-10} cm^3 (STP)-cm/cm^2-s-cm Hg; propane at 50.8 mm Hg pressure, 3.7×10^{-10}cm^3(STP)-cm/cm^2/s-cm Hg; and ethane at 50.9 mm Hg pressure, 0.92×10^{-9} cm^3 (STP)-cm/cm^2-s-cm Hg. The permeabilities obtained in this study at 30°C and 50 mm Hg pressure are as follows: *n*-butane, 4.47×10^{-10} cm^3(STP)-cm/cm^2-s-cm Hg; propane, 5.88×10^{-10} cm^3(STP)-cm/cm^2-s-cm Hg; and ethane, 1.262×10^{-9} cm^3(STP)-cm/cm^2-s-cm Hg.

The permeability of these three gases exhibits pressure dependency. For example, the permeability of *n*-butane at 30°C decreased from 5.6×10^{-10} to 4.407×10^{-10} cm^3(STP)-cm/cm^2-s-cm Hg with an increase in pressure from 25 to 200 mm Hg. Similarly, the permeability of propane and ethane at the same temperature and pressure decreased from 6.305×10^{-9} to

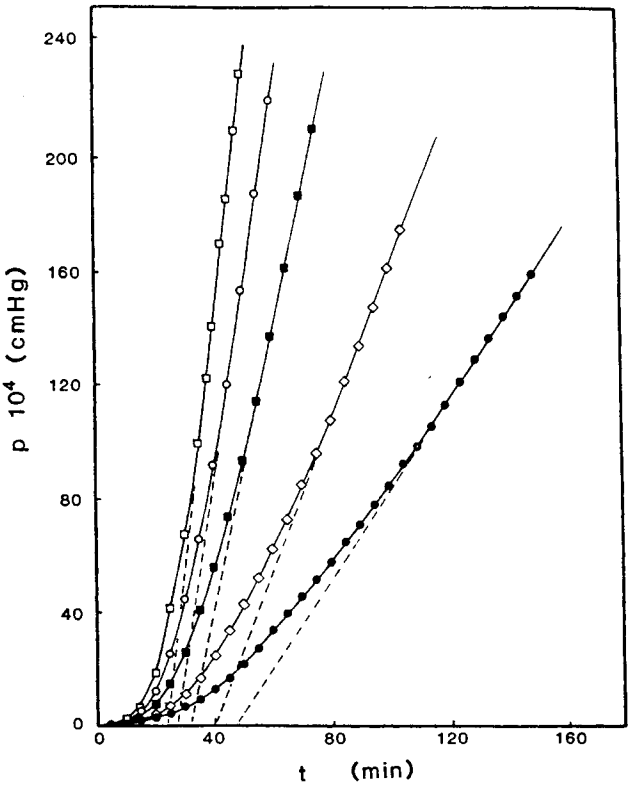

Fig. 2. Pressure versus time plot for *n*-butane through ethylcellulose at 40°C and various pressures; (●) 2.5 cm Hg; (◇) 5 cm Hg; (■) 10 cm Hg; (○) 15 cm Hg; (□) 20 cm Hg.

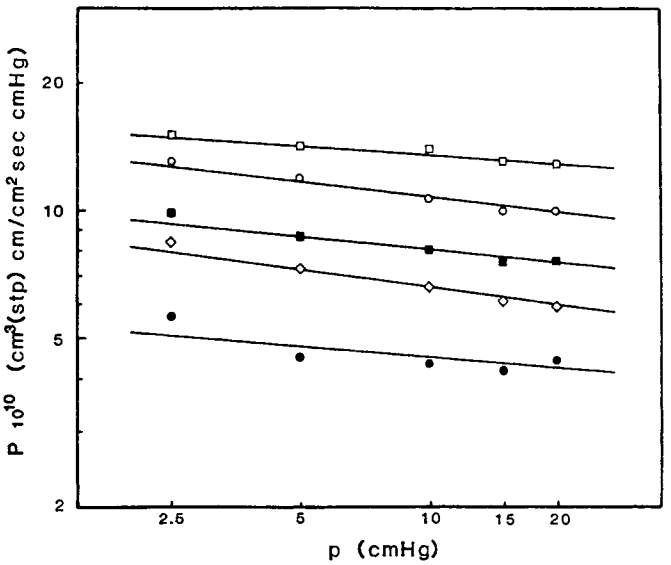

Fig. 3. Permeability coefficients of *n*-butane in ethylcellulose at various temperatures and pressures; (●) 30°C; (◇) 40°C; (■) 50°C; (○) 60°C; (□) 70°C.

4.540×10^{-10} cm^3(STP)-cm/cm^2-s-cm Hg and 1.333×10^{-9} to 1.157×10^{-9} cm^3(STP)-cm/cm^2-s-cm Hg, respectively. The pressure dependency of the permeabilities becomes smaller as the temperature increases. This decrease in permeability as the pressure increases and the lower dependency on pressure as the temperature increases toward the glass transition temperature has been reported by others.[16]

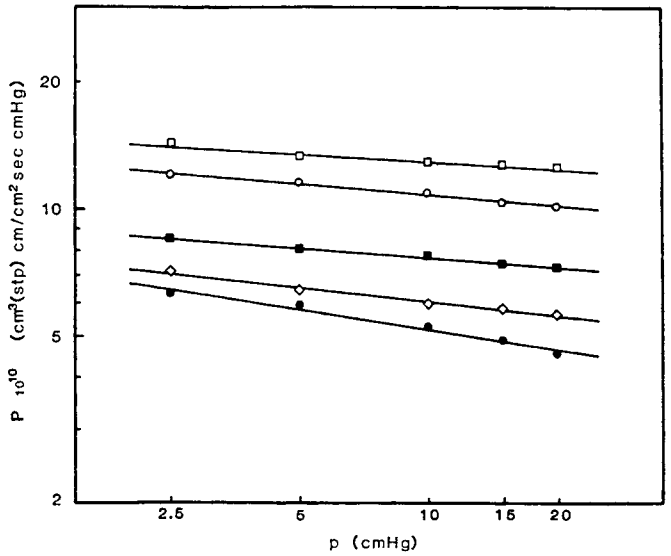

Fig. 4. Permeability coefficients of propane in ethylcellulose at various temperatures and pressures; (●) 30°C; (◇) 40°C; (■) 50°C; (○) 60°C; (□) 70°C.

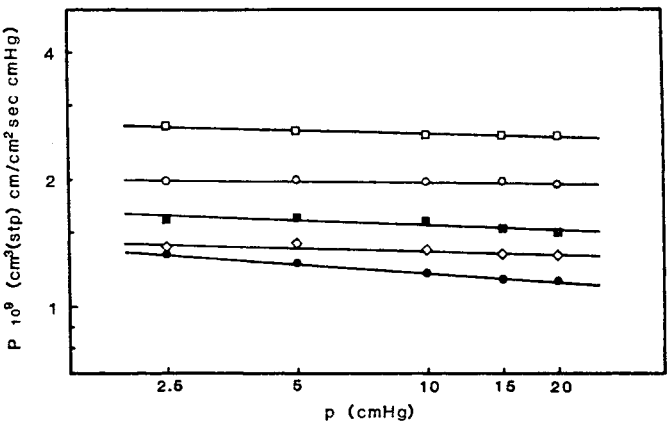

Fig. 5. Permeability coefficients of ethane in ethylcellulose at various temperatures and pressures; (●) 30°C; (◇) 40°C; (■) 50°C; (○) 60°C; (□) 70°C.

The decrease in permeability with pressure can be related to the complex sorption and diffusion mechanism of the glassy polymers. In the rubber state, where the temperature is above the glass transition temperature, the sorption mechanism follows Henry's law and the transport follows Fick's first law with a concentration-independent diffusion coefficient. The decrease in pressure dependency of the permeability with increasing temperature can be related to structural changes in the polymer and changes of the sorption and diffusion mechanism.[1]

Diffusion Time Lags

The observed diffusion time lags θ for each run were determined by extrapolation of the steady-state portion of the plot of pressure versus time to the time axis where $p = 0$. A linear least-squares analysis technique was applied to the steady-state portion of the plot to determine the time lags.

The measured time lags for *n*-butane, propane, and ethane at different upstream pressures and temperatures are illustrated in Figures 6 through 8, respectively. The strong dependence of the time lags on the upstream pressure, with the exception of ethylcellulose-ethane at 70°C, is shown in these figures. This pressure dependency of the time lag has been observed in other glassy polymer-penetrant systems.[12,16–18] The decrease in time lag with increasing pressure (i.e., concentration) is greatest for *n*-butane. This may be due to the high penetrant solubility and therefore greater plasticization effect for *n*-butane with respect to propane or ethane.[1]

Analysis of Permeabililty Data

A simple model that describes mass transfer in rubber or high polymers above their glass transition temperature follows Henry's law for sorption and Fick's first law with a concentration-independent diffusion coefficient.

TABLE I
Permeabilities in Ethylcellulose at Various Pressures and Temperatures[a]

	Temp (°C)	2.5 cm Hg	5 cm Hg	10 cm Hg	15 cm Hg	20 cm Hg
n-Butane	30	$5.599\ 10^{-10}$	$4.470\ 10^{-10}$	$4.328\ 10^{-10}$	$4.162\ 10^{-10}$	$4.407\ 10^{-10}$
	40	$8.396\ 10^{-10}$	$7.250\ 10^{-10}$	$6.515\ 10^{-10}$	$6.013\ 10^{-10}$	$5.867\ 10^{-10}$
	50	$9.905\ 10^{-10}$	$8.583\ 10^{-10}$	$8.000\ 10^{-10}$	$7.501\ 10^{-10}$	$7.547\ 10^{-10}$
	60	$13.020\ 10^{-10}$	$11.780\ 10^{-10}$	$10.630\ 10^{-10}$	$9.890\ 10^{-10}$	$9.890\ 10^{-10}$
	70	$15.220\ 10^{-10}$	$14.100\ 10^{-10}$	$13.800\ 10^{-10}$	$12.930\ 10^{-10}$	$12.870\ 10^{-10}$
Propane	30	$6.305\ 10^{-10}$	$5.880\ 10^{-10}$	$5.249\ 10^{-10}$	$4.880\ 10^{-10}$	$4.540\ 10^{-10}$
	40	$7.091\ 10^{-10}$	$6.394\ 10^{-10}$	$5.976\ 10^{-10}$	$5.810\ 10^{-10}$	$5.626\ 10^{-10}$
	50	$8.482\ 10^{-10}$	$8.022\ 10^{-10}$	$7.713\ 10^{-10}$	$7.389\ 10^{-10}$	$7.275\ 10^{-10}$
	60	$12.070\ 10^{-10}$	$11.530\ 10^{-10}$	$10.900\ 10^{-10}$	$10.340\ 10^{-10}$	$10.130\ 10^{-10}$
	70	$14.330\ 10^{-10}$	$13.310\ 10^{-10}$	$12.680\ 10^{-10}$	$12.670\ 10^{-10}$	$12.560\ 10^{-10}$
Ethane	30	$13.330\ 10^{-10}$	$12.620\ 10^{-10}$	$11.970\ 10^{-10}$	$11.630\ 10^{-10}$	$11.570\ 10^{-10}$
	40	$13.780\ 10^{-10}$	$14.070\ 10^{-10}$	$13.670\ 10^{-10}$	$13.360\ 10^{-10}$	$13.190\ 10^{-10}$
	50	$16.220\ 10^{-10}$	$16.310\ 10^{-10}$	$15.900\ 10^{-10}$	$15.370\ 10^{-10}$	$14.950\ 10^{-10}$
	60	$19.820\ 10^{-10}$	$19.980\ 10^{-10}$	$19.660\ 10^{-10}$	$19.750\ 10^{-10}$	$19.410\ 10^{-10}$
	70	$26.860\ 10^{-10}$	$26.120\ 10^{-10}$	$25.580\ 10^{-10}$	$25.450\ 10^{-10}$	$25.370\ 10^{-10}$

[a] P = cm^3cc (STP) cm/cm^2 -s-cm Hg.

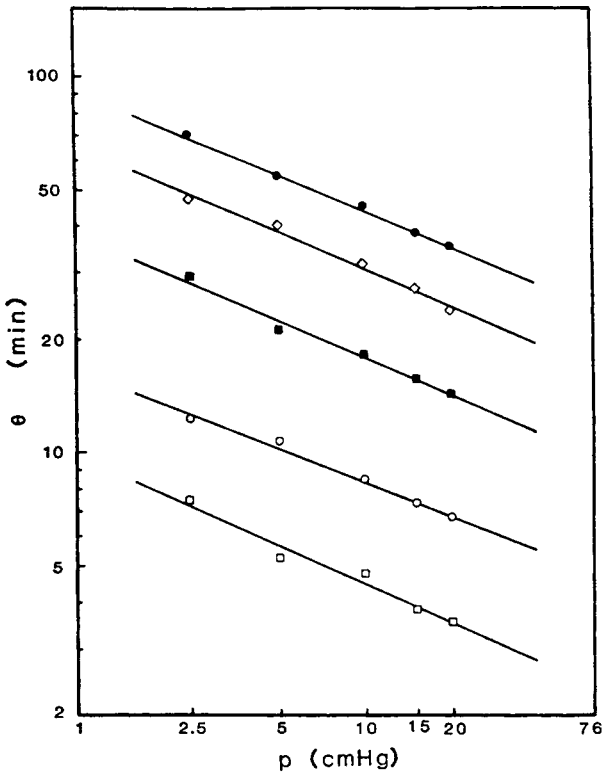

Fig. 6. *n*-Butane diffusion time lag in ethylcellulose at various temperatures; (●) 30°C; (◇) 40°C; (■) 50°C; (○) 60°C; (□) 70°C. Film thickness: 0.00409 cm at 30°C and 0.00483 cm at other temperatures.

In this case, permeability and the diffusion time lag are expressed by eqs. (6) and (7), respectively:

$$P = k_D D \tag{6}$$

$$\theta = \frac{l^2}{6D} \tag{7}$$

and are independent of upstream gas pressure. These parameters are temperature dependent.

Mass transfer in glassy polymers is more complex than rubbery polymers, primarily because of the more complex structural state of glassy polymers. However, mathematical models have been developed and the formulation of the dual sorption effect on the time lag and permeability of the glassy polymers has been reported.[7] The total immobilization model assumes that the gas sorbed by the Langmuir mode is totally immobilized and therefore does not contribute to the diffusive flux. For the total immobilization model, permeability has the form of eq. (6) and the time lag has the form of eq. (4). In this case, permeability is independent of upstream gas pressure but the time lag is pressure dependent. For the partial immobilization model,

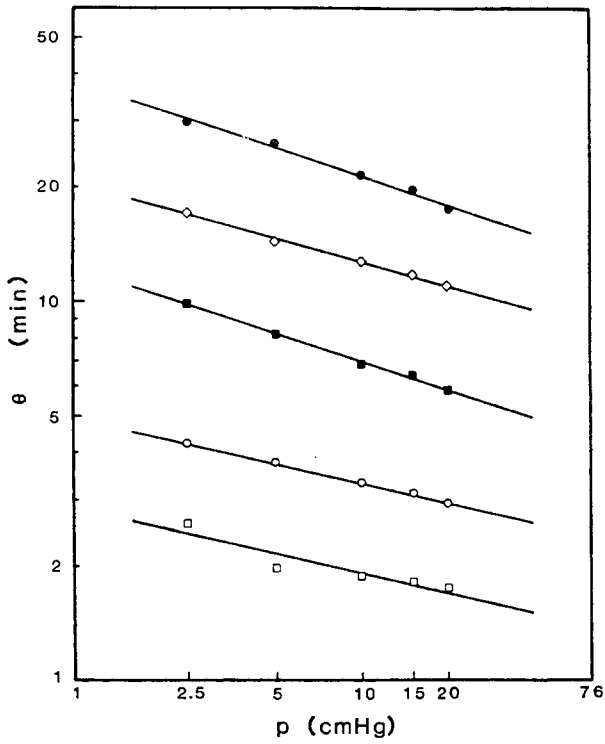

Fig. 7. Propane diffusion time lag in ethylcellulose at various temperatures; (●) 30°C; (◇) 40°C; (■) 50°C; (○) 60°C; (□) 70°C. Film thicknesses: 0.00483 cm.

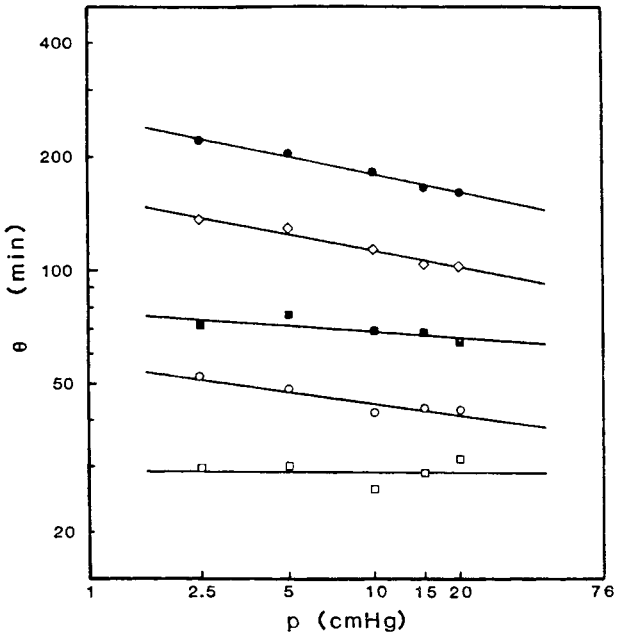

Fig. 8. Ethane diffusion time lag in ethylcellulose at various temperatures; (●) 30°C; (◇) 40°C; (■) 50°C; (○) 60°C; (□) 70°C. Film thickness: 0.00483 cm.

the permeability and the diffusion time lag are described by eqs. (8) and (9), respectively:

$$P = k_D D \left(1 + \frac{FK}{(1 + bp)}\right) \tag{8}$$

$$\frac{6D\theta}{l^2} = \frac{1 + K[f_0 + FKf_1 + (FK)^2 f_2] + FKf_3 + (FK)^2 f_4}{\left(1 + \frac{FK}{1 + y}\right)^3} \tag{9}$$

where

$$f_0 = \frac{6}{y^3}\left[\frac{y^2}{2} = y - (1 + y)\ln(1 + y)\right]$$

$$f_1 = \frac{6}{y^3}\left[\frac{y}{2} - \frac{3y}{2(1 + y)} + \frac{\ln(1 + y)}{1 + y}\right]$$

$$f_2 = \frac{6}{y^3}\left[\frac{1}{6} - \frac{1}{2(1 + y)} + \frac{1}{2(1 + y)^2} - \frac{1}{6(1 + y)^3}\right]$$

$$f_3 = \frac{6}{y^3}\left[-\frac{3}{2}y + \frac{y}{2(1 + y)} + (1 + y)\ln(1 + y)\right]$$

$$f_4 = \frac{6}{y^3}\left[\frac{1}{2} - \frac{1}{2(1 + y)^2} - \frac{\ln(1 + y)}{1 + y}\right]$$

The assumption employed in the development of the partial immobilization model are as follows[9,10]:

1. The sorption mechanism is described by the dual sorption model.
2. Local equilibrium is always maintained between gas molecules in the different sorption modes C_D and C_H.
3. The gases sorbed by the two modes can have a finite diffusional mobility characterized by constant diffusion coefficients D_D and D_H.

where $F = D_H/D_D$, D_D and D_H are the diffusion coefficients of the Henry's law and Langmuir populations, respectively.

In this case, both the permeability and time lag are pressure dependent. The partial immobilization model has two limitations. One is the assumption of total immobilization of the Langmuir species, and the other is the equal mobility (no immobilization) of the Henry's law and the Langmuir-mode species. For no immobilization, the time lag is expressed by eq. (7) and the permeability can be represented by eq. (8). In this case, the time lag is constant and the permeability is very pressure dependent.

The permeability and time lag results shown in Figures 3 through 8 show pressure dependency. Therefore, the partial immobilization model was used to analyze the permeability data.

The plots of experimentally determined permeabilities versus $1/(1 + bp)$ are shown in Figures 9 through 11. The linearity of data in these figures

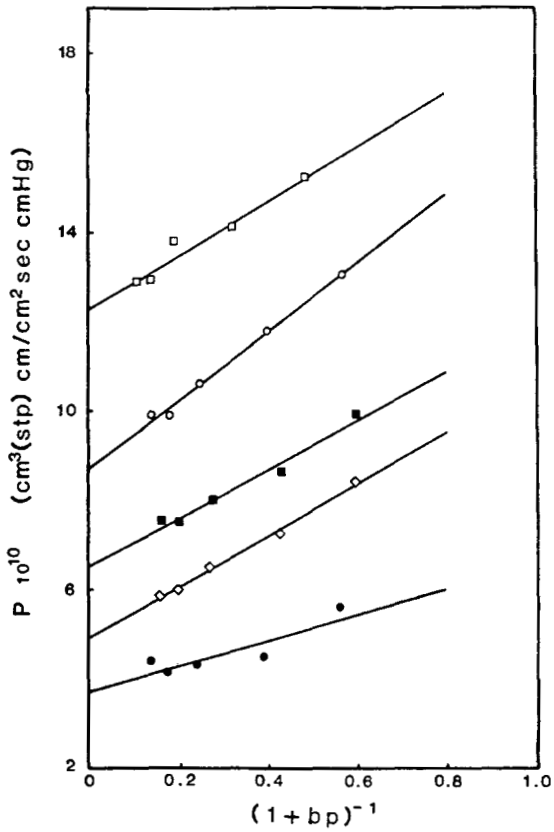

Fig. 9. n-Butane permeability in ethylcellulose at various temperatures plotted according to eqs. (3) through (42); (●) 30°C; (◇) 40°C; (■) 50°C; (○) 60°C; (□) 70°C.

is consistent with eq. (8). From the slopes and intercepts of the solid lines, the two partial immobilization parameters D_D and F were evaluated. Values of D_D, D_H, and F for n-butane, propane, and ethane are tabulated in Table II. The permeabilities are calculated from eq. (8) by using the transport parameters from Table II and the sorption parameters from Reference 1. In Figures 12 through 14, the solid lines are the prediction of the permeabilities from eq. (8) and the points are the experimental permeabilities. The pressure dependency of the permeabilities are well represented by the parial immobilization model.

The pressure dependency of the pemeability coefficient arises from the nonequilibrium character of the glassy state, and its magnitude is proportional to the contribution of the Langmuir-mode sorption and the diffusivity of these species. At low pressure this contribution is maximized. As $p \rightarrow 0$, eq. (8) reduces to the expression

$$\lim_{p \rightarrow 0} P = k_D D_D + C'_H b D_H \tag{10}$$

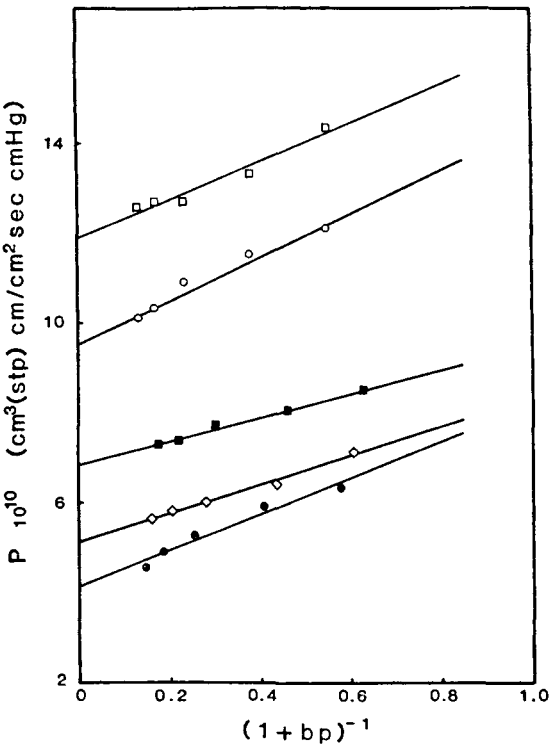

Fig. 10. Propane permeability in ethylcellulose at various temperatures plotted according to eqs. (3) through (42); (●) 30°C; (◇) 40°C; (■) 50°C; (○) 60°C; (□) 70°C.

At high pressures, as $p \rightarrow \infty$, the expression becomes

$$\lim_{p \rightarrow 0} P = k_D D_D \tag{11}$$

where the contribution of the Langmuir mode is zero. At both extremes the permeability is constant and varies with pressure between these limits. The permeability of *n*-butane, propane, and ethane at low- and high-pressure limits are given in Table III.

The partial immobilization model has been applied to various glassy polymer-penetrant systems.[11,13,16,17,19] The diffusion coefficient of the Langmuir species D_H in these polymer-penetrant systems were found to be much lower than the diffusivity of the Henry's law species D_D.

In this study, no consistent trend was observed relating temperature with the degree of immobilization. The F values shift toward the one limit of the partial immobilization (i.e., no immobilization or equal mobility of the two modes) as the gas changes from C_4 to C_2 hydrocarbons. This behavior may be attributed to a decrease in gas solubility in ethylcellulose and a decrease in the Lennard-Jones force constant as the gas changes from C_4 to C_2 hydrocarbons.

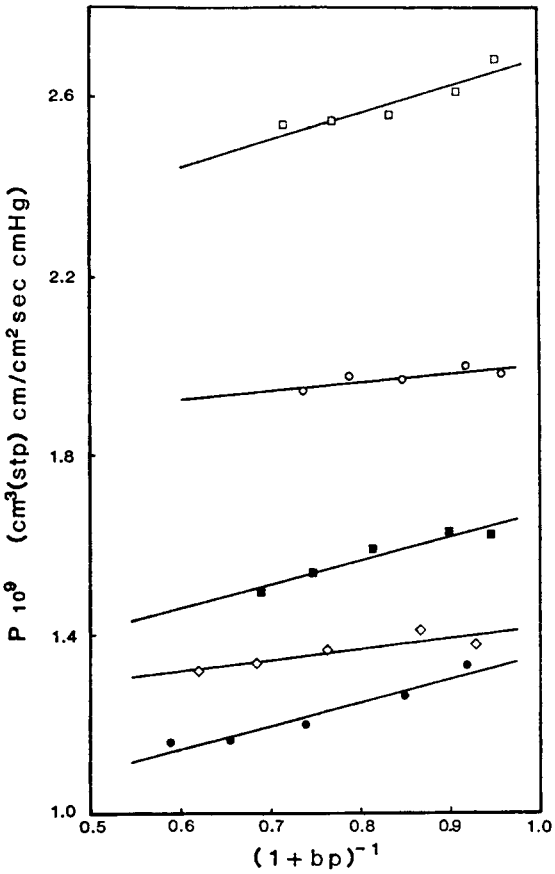

Fig. 11. Ethane permeability in ethylcellulose at various temperatures plotted according to eqs. (3) through (42); (●) 30°C; (◇) 40°C; (■) 50°C; (○) 60°C; (□) 70°C.

TABLE II
n-Butane, Propane, and Ethane Transport Parameters for Ethylcellulose at Various Temperatures

	Temperature (°C)	D_D (cm²/s)	D_H (cm²/s)	F
n-Butane	30	$1.631\ 10^{-9}$	$2.484\ 10^{-10}$	0.1523
	40	$2.612\ 10^{-9}$	$8.030\ 10^{-10}$	0.3074
	50	$3.987\ 10^{-9}$	$12.860\ 10^{-10}$	0.3225
	60	$6.042\ 10^{-9}$	$31.070\ 10^{-10}$	0.5143
	70	$10.411\ 10^{-9}$	$39.060\ 10^{-10}$	0.3752
Propane	30	$3.121\ 10^{-9}$	$2.852\ 10^{-9}$	0.9140
	40	$5.051\ 10^{-9}$	$4.136\ 10^{-9}$	0.8188
	50	$8.895\ 10^{-9}$	$5.123\ 10^{-9}$	0.5760
	60	$15.710\ 10^{-9}$	$14.720\ 10^{-9}$	0.9370
	70	$24.070\ 10^{-9}$	$14.570\ 10^{-9}$	0.6053
Ethane	30	$1.733\ 10^{-8}$	$4.362\ 10^{-8}$	2.517
	40	$3.109\ 10^{-8}$	$2.624\ 10^{-8}$	0.844
	50	$3.876\ 10^{-8}$	$7.810\ 10^{-8}$	2.015
	60	$7.309\ 10^{-8}$	$3.771\ 10^{-8}$	0.516
	70	$10.516\ 10^{-8}$	$13.850\ 10^{-8}$	1.317

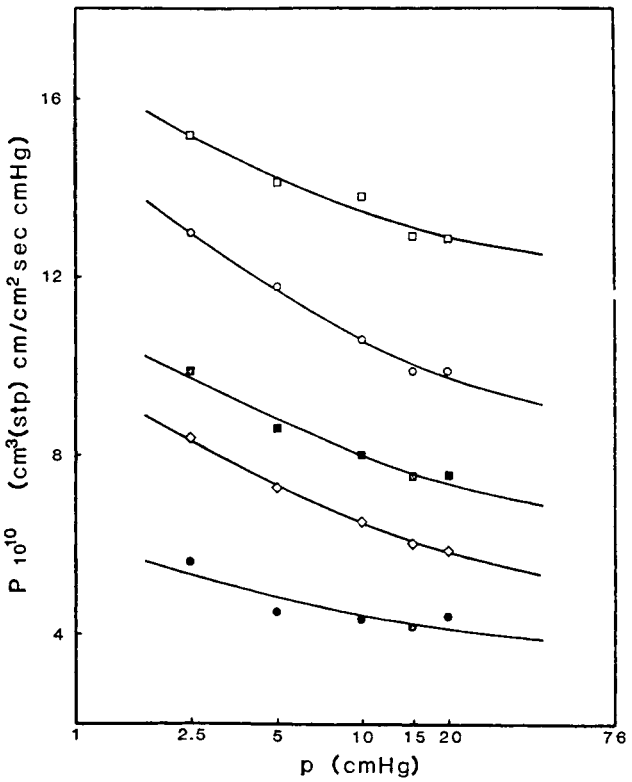

Fig. 12. Comparison of partial immobilization model predictions of n-butane permeability in ethylcellulose with experimental data; (●) 30°C; (◇) 40°C; (■) 50°C; (○) 60°; (□) 70°C.

Paul and Koros[10] have pointed out that two different physical meanings can be assigned to F. One interpretation is that the gases dissolved by the Henry's law mode and the Langmuir mode are fully mobile but they have different mobilities and are characterized by the diffusion coefficients D_D and D_H, respectively. The parameter F represents the relative mobility of the two modes $F = D_H/D_D$. The other interpretation is that the gas dissolved by the Henry's law mode and a fraction F of the gas dissolved by the Langmuir mode have the same mobility and are characterized by the diffusion coefficient D_D. The concentration of the mobile part is given below.

$$C_m = C_D + FC_H = C_D\left(1 + \frac{FK}{(1 + aC_D)}\right) \tag{12}$$

The remaining fraction $(1 - F)$ of the gas sorbed by the Langmuir mode is assumed to be totally immobilized. The flux equations resulting from the first and second interpretation are given by eqs. (13) and (14), respectively.

$$J = -D_D \frac{\delta C_D}{\delta x} - D_H \frac{\delta C_H}{\delta x} \tag{13}$$

$$J = -D \frac{\delta C_m}{\delta x} \tag{14}$$

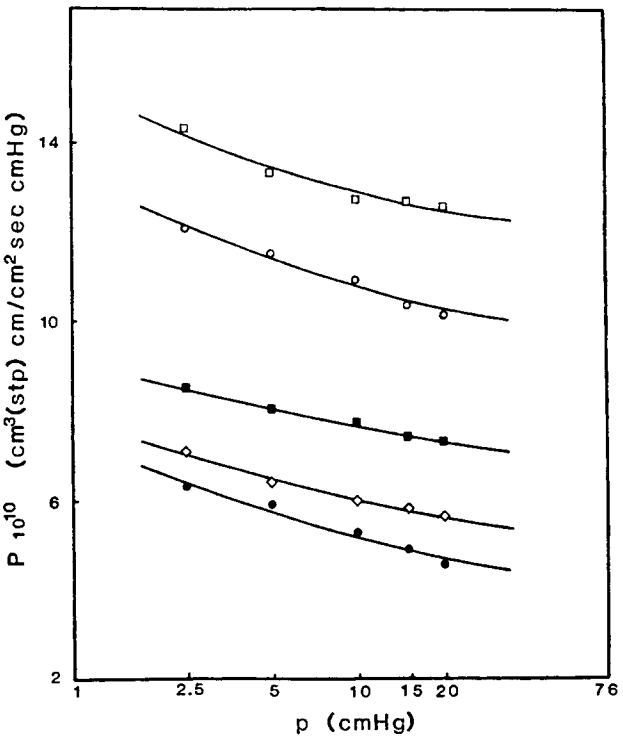

Fig. 13. Comparison of partial immobilization model predictions of propane permeability in ethylcellulose with experimental data; (●) 30°C; (◇) 40°C; (■) 50°C; (○) 60°C; (□) 70°C.

In the formulation of the partial immobilization model, the diffusion coefficients were assumed to be constant. Paul and Koros[10] have shown that when the diffusion coefficients are constant, the two relations for F and eqs. (13) and (14) yield the same result. If the diffusion coefficients are concentration dependent, the two interpretations of the partial immobilization model yield different analytical results. Fluctuations of F with the temperature may be the result of the concentration dependencies of the diffusion coefficients.

One of the limiting cases of the partial immobilization model is that of no immobilization. The equal mobility of the two sorption species requires that $F = D_H/D_D$ be equal to 1. The equal mobility assumption rules out the possibility of the diffusivity of the Langmuir species D_H being greater than the diffusivity of the Henry's law species D_D. The F values of ethane at 30, 50, and 70°C were found to be greater than 1. The concentration of the mobile part C_m calculated from eq. (12) with these F values yields C_m values calculated from eq. (12) with these F values yields C_m values greater than the total concentration of the ethane in ethylcellulose, which is physically impossible. If one assumes that $F > 1$ "is possibly not statistically different from one"[17] the time lag has to be a constant and the permeability pressure dependent.[10] The time lag data in Figure 8 are pressure dependent except at 70°C, and the pressure dependency of the permeabilities at 30, 50, and 70°C are well described by the partial immobilization formulation eq. (8) with values of F greater than 1.

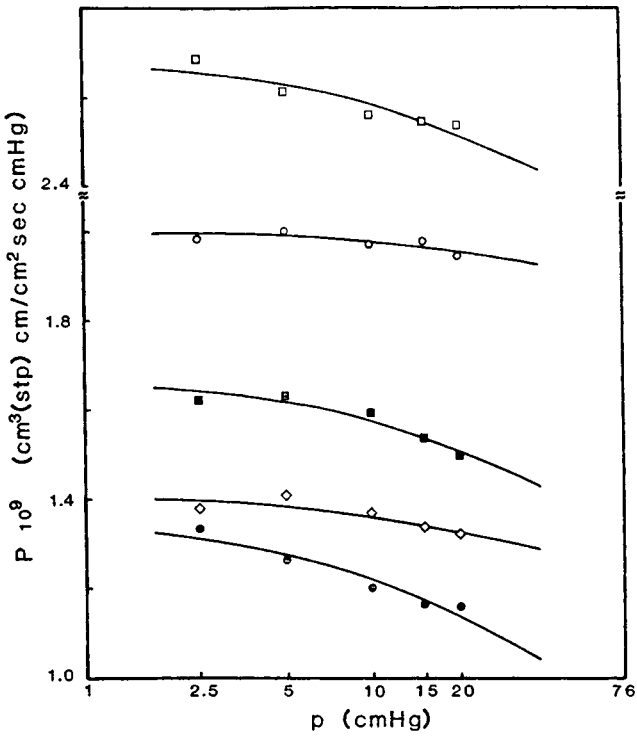

Fig. 14. Comparison of partial immobilization model predictions of ethane permeability in ethylcellulose with experimental data; (●) 30°C; (◇) 40°C; (■) 50°C; (○) 60°C; (□) 70°C.

TABLE III
High- and Low-Pressure Limits of *n*-Butane, Propane, and Ethane Permeability for Ethylcellulose at Various Temperatures[a]

	Temperature (°C)	$P(\infty) = k_D D_D$	$P(0) = k_D D_D + C_H' b D_H$
n-Butane	30	$3.723\ 10^{-10}$	$6.610\ 10^{-10}$
	40	$4.921\ 10^{-10}$	$10.600\ 10^{-10}$
	50	$6.519\ 10^{-10}$	$11.880\ 10^{-10}$
	60	$8.695\ 10^{-10}$	$16.850\ 10^{-10}$
	70	$12.296\ 10^{-10}$	$18.320\ 10^{-10}$
Propane	30	$4.117\ 10^{-10}$	$8.097\ 10^{-10}$
	40	$5.112\ 10^{-10}$	$8.281\ 10^{-10}$
	50	$6.845\ 10^{-10}$	$9.452\ 10^{-10}$
	60	$9.635\ 10^{-10}$	$14.280\ 10^{-10}$
	70	$11.870\ 10^{-10}$	$16.090\ 10^{-10}$
Ethane	30	$8.246\ 10^{-10}$	$13.548\ 10^{-10}$
	40	$11.740\ 10^{-10}$	$14.156\ 10^{-10}$
	50	$11.430\ 10^{-10}$	$16.700\ 10^{-10}$
	60	$18.120\ 10^{-10}$	$20.000\ 10^{-10}$
	70	$20.980\ 10^{-10}$	$26.840\ 10^{-10}$

[a] P = cm³ (STP) cm/cm²-s-cm Hg.

The composite permeability coefficient is the product of the solubility and the diffusivity of the penetrant gas. Both the solubility and the diffusion coefficient depend not only on the characteristics of the gas but also on the polymer characteristics. A principal characteristic of the penetrant gas that influences the diffusivity is the size of the penetrant molecule. The diffusion of the penetrant through the polymer matrix largely depends upon the availability of polymer free volume to permit the passage of the penetrant. If the fractional free volume of the polymer is large, the diffusion coefficient is large and the dependence of the diffusion coefficient is large and the dependence of the diffraction coefficient on penetrant size is small.[20] Because of restricted synchronized rotation of polymer chain segments, the fractional free volume in the glassy state is smaller than in the rubber state. Meares[21] has suggested that the formation of free volume in the glassy state occurs by reduction of the van der Walls bonds between chain segments. If chain separations are larger than the diameter of gas molecules, an activated diffusion process takes place as a result of successive jumps of the penetrant molecules from one absorption site to another. As the size of the penetrant increases, the displacement of a penetrant molecules depends upon rotation of chain segments and the availability of voids larger than the penetrant size, and as a result a small change in penetrant size can result in a substantial change in diffusivity. As the temperature increases, the amplitude of the segmental oscillations of the polymer chain also increases. Greater segmental motion results in an increase in the size of voids and an increase diffusivity as the temperature increases.

Variation in the diffusion coefficient of the Henry's law species D_D with the molecular size of n-butane, propane, and ethane at different temperatures is shown in Figure 15. In this correlation, the Lennard-Jones collision diameter of the penetrant molecule is used.[22] At a constant temperature D_D decreases the penetrant size increases. At 30 and 70°C, for instance, there is a 10-fold increase in D_D as the penetrant is changed from n-butane to ethane. Figure 15 also represents the correlation of the concentration-dependent diffusion coefficient at the high-pressure limit, where the Langmuir sorption contribution is zero. Similar correlations for other glassy polymer-penetrant systems have been reported.[17,19,23]

The diffusivity of the Langmuir species D_H could not be correlated with penetrant size. This lack of correlation of D_H with d may be due to the different diffusion mechanism for the Langmuir species. The diffusion of normally dissolved species D_D is associated with the segmental motion of chain segments, the availability of free volume to accomodate the penetrant molecules, and, therefore, depends upon the penetrant size, as shown in Figure 15. D_H represents the diffusivity of gases that absorb in microvoids of the glassy state by Langmuir-type absorption. In the rubbery state and in the case of total immobilization, D_H is zero, because of the disappearance of the microvoids and the total immobilization of the sorbed species. A lack of correlation of D_H with d suggests that the penetrant size has little or no effect on D_H.

Chen and Edin[24] have employed the following equation, which is based on the free-volume theory of diffusion[25] and Meares' model,[21] to correlate the diffusion coefficients of alkanes in glassy polycarbonate at low penetrant concentration.

$$\ln D = \ln A - (b\pi\lambda/4v)d^2 \tag{15}$$

where A is a constant, b is a geometric constant, λ is the length of a diffusion step, and v is the average free volume available per polymer segment at a given temperature. A similar correlation has been presented for various gases in PET.[26]

At zero penetrant concentration, the effective diffusivity can be written as

$$D_{\text{eff}}(0) = D_D\left[\frac{1 + FK}{1 + K}\right] \tag{16}$$

At the limit, $D_{\text{eff}}(0)$ is independent of concentration and the effect of the Langmuir mode of sorption is a maximum. The diffusivities of both species contribute to $D_{\text{eff}}(0)$. In Figure 16, $D_{\text{eff}}(0)$ is plotted versus d^2 according to eq. (15). The ln $D_{\text{eff}}(0)$ varies linearly with d^2 at five temperatures, with a change in $D_{\text{eff}}(0)$ of about three orders of magnitude.

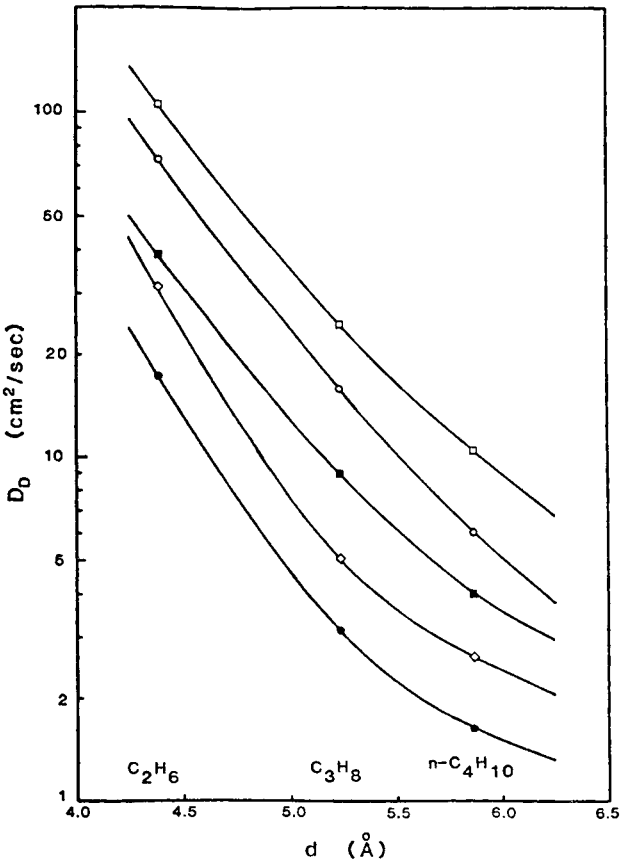

Fig. 15. Correlation of D_D in ethylcellulose with the molecular diameter of penetrant gas at various temperatures; (●) 30°C; (◇) 40°C; (■) 50°C; (○) 60°C; (□) 70°C.

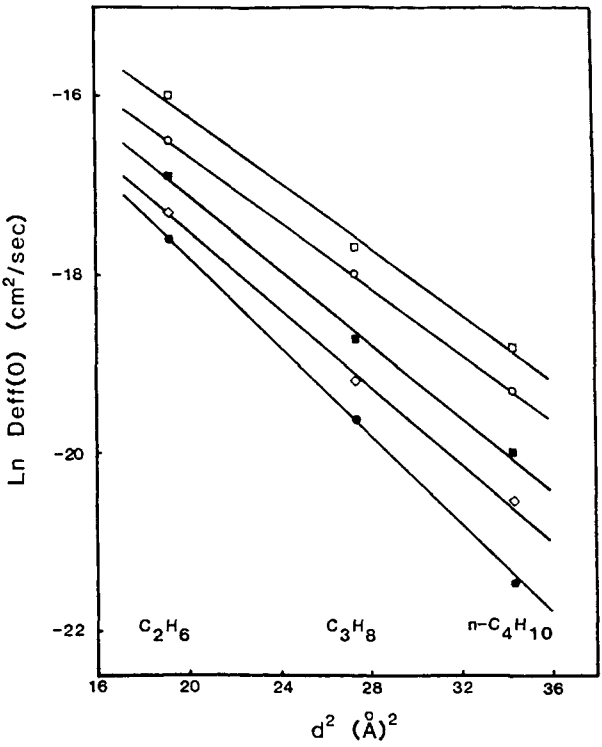

Fig. 16. Correlation of effective diffusion coefficient at zero concentration with the square of penetrant molecular diameters; (●) 30°C; (◇) 40°C; (■) 50°C; (○) 60°C; (□) 70°C.

Effective Diffusion Coefficient

If the interaction between the polymer and penetrant does not affect the morphology of the polymer, the diffusion coefficient will not be a function of concentration. The flux of the penetrant at constant temperature is given by Fick's first law with a constant diffusion coefficient. For many polymer-penetrant systems, the diffusion coefficient exhibits concentration dependence because of plasticization and the swelling effect of the penetrant. For this case, the concentration dependent diffusion coefficient increases with concentration.

For glassy polymers, the concentration dependence of the diffusion coefficient arises from different mobilities of the species sorbed by the two sorption modes. The flux of penetrant for the partial immobilization model is given by

$$J = -D\left[\frac{1+\dfrac{FK}{(1+aC_D)^2}}{1+\dfrac{K}{(1+aC_D)^2}}\right]\frac{\delta C}{\delta x} \tag{17}$$

An analytic expression for the concentration-dependent diffusion coefficient can be developed from eq. (17) and Fick's first law.

$$D_{\text{eff}} = D\left[\frac{1 + \dfrac{Fk}{(1 + aC_D)^2}}{1 + \dfrac{K}{(1 + aC_D)^2}}\right] \tag{18}$$

Equation (18) is the formulation of the concentration-dependent diffusion coefficient D_{eff} according to the partial immobilization model.

Although D_{eff} can be predicted from the partial immobilization model with the aid of sorption and transport parameters it also can be determined independently from experimental results. The following equation was employed to determine the concentration dependent diffusion coefficient $D(C)$ from the sorption isotherm and the pemeability data by using graphic differentiation.[12]

$$D(C) = \left(P(p) + P\frac{dP}{dp}\right)\left(\frac{\delta p}{\delta C}\right)_p \tag{19}$$

The solid lines in Figures 17 through 19 are determined from eq. (18) by using the sorption and transport parameters from Reference 1 and Table II, respectively. The points in these figures are calculated from eq. (19) by using the appropriate sorption isotherm and permeation data. A good correlation between the theoretical prediction and the experimental results indicates that the concentration dependence of the diffusion coefficient in glassy polymers can be explained by the partial immobilization model.

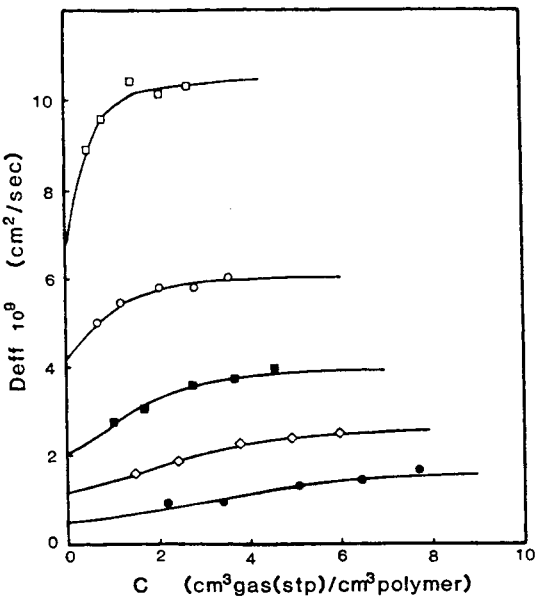

Fig. 17. Effective concentration-dependent diffusion coefficient for *n*-butane in ethylcellulose at various temperatures; (●) 30°C; (◇) 40°C; (■) 50°C; (○) 60°C; (□) 70°C.

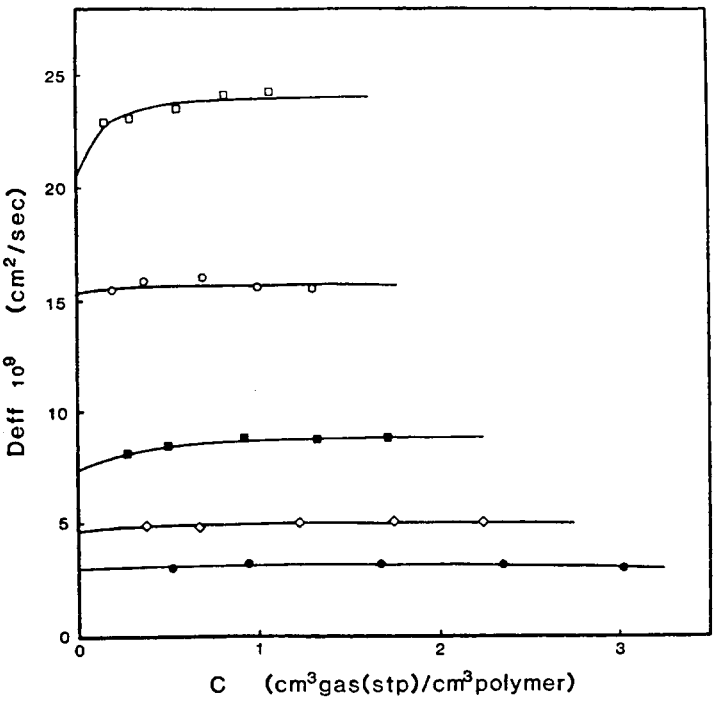

Fig. 18. Effective concentration-dependent diffusion coefficient for propane in ethylcellulose at various temperatures; (●) 30°C; (◇) 40°C; (■) 50°C; (○) 60°C; (□) 70°C.

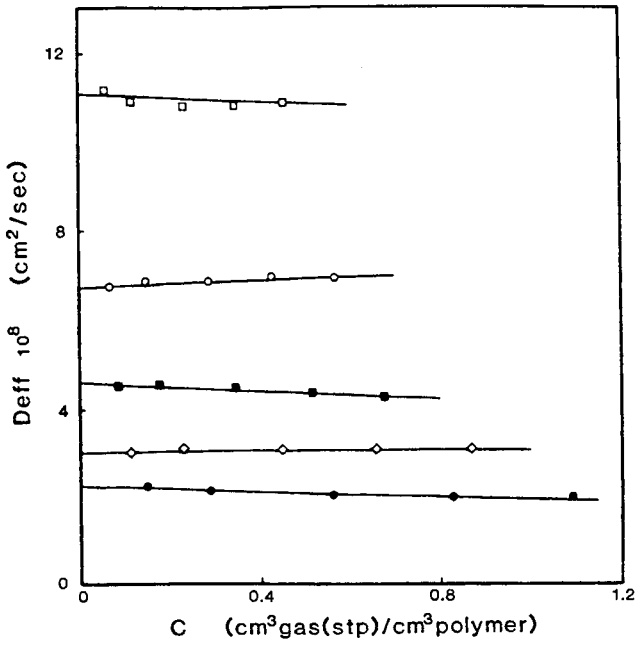

Fig. 19. Effective concentration-dependent diffusion coefficient for ethane in ethylcellulose at various temperatures; (●) 30°C; (◇) 40°C; (■) 50°C; (○) 60°C; (□) 70°C.

The concentration dependence of the diffusion coefficient is proportional to the amount of gas immobilized and the diffusivities of the two sorption species, or the degree of immobilization. The factor $K = C'_H b/k_D$, is a measure of the quantity of penetrant absorbed in microvoids relative to the amount normally dissolved in the polymer. Because of a significant reduction in C'_H, K becomes smaller as the temperature increases. Therefore, D_{eff} in eq. (18) becomes less concentration dependent. This behavior is well represented in Figure 17. The reduction in the value of K for n-butane is about a factor of 4 between 30 and 70°C. At low temperatures, for example, 30 and 40°C, the effect of concentration on D_{eff} is not significant at low concentration. The initial sharp increase in D_{eff} at high temperatures is believed to be caused by the plasticization effect of n-butane. At high temperatures, a small quantity of highly soluble n-butane plasticizes the ethylcellulose, reduces the glass transition temperature, and increases the diffusion coefficient. Beyond a certain concentration of penetrant, of about 2 and 1 cm^3(STP)/cm^3 polymer at 60 and 70°C, respectively, D_{eff} remains almost constant. Propane, which is less soluble than n-butane in ethylcellulose, begins to plasticize the polymer and affect D_{eff} only at 70°C.

The value of K depends upon the type of penetrant, as well as the temperature. As the penetrant gas changes from n-butane to propane to ethane, the K values become smaller and variations of D_{eff} with concentration become negligible, as shown in Figures 17 through 19.

The effective diffusion coefficient is concentration dependent between the low- and high-pressure limits. As $p \rightarrow 0$ (i.e., $C = 0$), eq. (18) has the form of eq. (16), and at high pressures as $p \rightarrow \infty$, eq. (18) reduces to $D_{\text{eff}} = D_D$. In both cases, D_{eff} is constant. D_{eff} varies between these limits at intermediate concentrations, as shown in Figures 17 and 18, and reaches a maximum constant value of D_D at high concentrations. A comparison of D_{eff} and D_D values for n-butane and propane in Figures 17 and 18 suggests that D_{eff} approaches D_D at low concentrations as K becomes smaller. The other variable that has a significant effect on D_{eff} is F. In the case of the equal mobility model, where $F = 1$, eq. (18) reduces to $D_{\text{eff}} = D_D$ and becomes independent of concentration. The F values for ethane at 30, 50, and 70°C are greater than 1, and the values of concentration-independent D_{eff} at these temperatures are shown in Figure 19. At 40 and 60°C, the F values are less than 1, but very small values of K at these temperatures make the concentration dependence of D_{eff} negligible.

The concentration dependence of the diffusion coefficient in other glassy polymer-penetrant systems[11,12,16,27] have been correlated by eq. (18). The strong concentration dependency of the diffusion coefficient in these systems has been attributed to the low mobility of the Langmuir-mode species.[16,17]

Temperature Dependence of Transport Parameters

Additional information the mechanism of diffusion and permeation can be obtained from the variation of the transport parameters with temperature. The variation of permeability and diffusion coefficients with temperature is expressed by equations of the Arrhenius type. The diffusion

coefficient and the activation energy of diffusion for concentration dependent systems are generally analyzed at the zero concentration limit. The diffusion coefficients at zero concentration were calculated from eq. (16) and plotted in Figure 20. The Arrhenius-type temperature dependence was obeyed by the three penetrants between the temperature range of 30 to 70°C. The activation energies E_D and the pre-exponential factors D_0 were obtained from these plots and are presented in Table IV.

The activation energy of diffusion is considered the energy required to complete the unit diffusion process of 1 mol of diffusing gas. An increase in E_D has been attributed either to an increase in the zone size if the energy required per chain separation is constant.[28] For a number of gas-polymer systems,[21,26,29-31] it has been observed that the activation energy of diffusion is greater in the rubbery state than in the glassy state. The length of diffusion steps were found to be much higher in the rubber state.[21,29] A high activation energy in the rubbery state, where larger zones of activation are involved, is the result of large jump distances associated with increased segmental mobility in the rubbery state. Since the jump distance is independent of penetrant size, the zone size essentially remains constant in either state of the polymer. The activation energy of diffusion is the energy required per chain separation for the diffusing molecule to pass, and an increase in E_D with penetrant size might be expected.

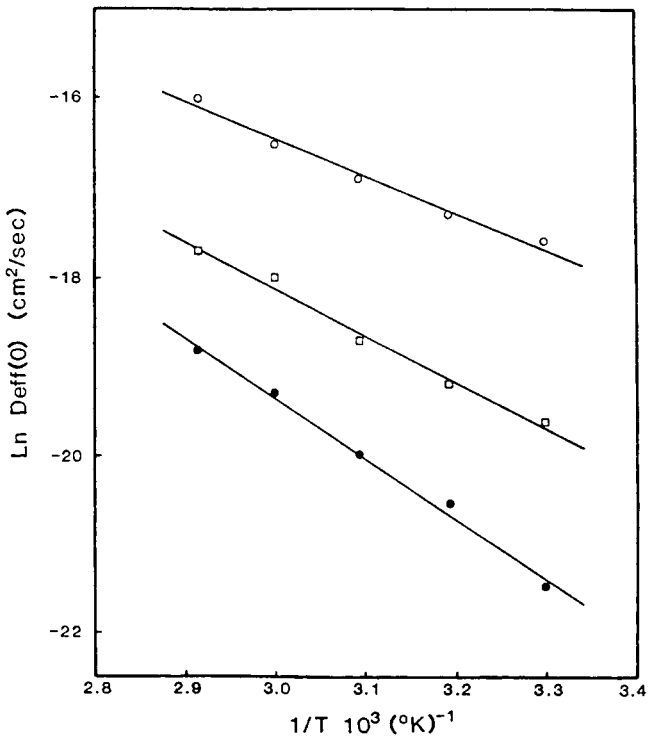

Fig. 20. Arrhenius plots of effective diffusion coefficients at zero concentration; (●) *n*-butane; (□) propane; (○) ethane.

TABLE IV
Activation Energy of Diffusion, Pre-exponential Factor, Molecular Diameter Jump Distance, and Entropy of Activation for *n*-Butane, Proane, and Ethane in Ethylcellulose

	d (Å)	E_D (cal/gmol)	D_o (cm^2/s)	λ (Å)	ΔS^* (cal/mol-K)	E_D (cal/mol)	D_o (cm^2/s)	E_H (cal/mol)	D_o (cm^2/s)
n-Butane	5.869	13,516	2.908	7.82	6.63	9,335	$8.581\ 10^{-3}$	14,215	5.42
Propane	5.240	10,373	$8.572\ 10^{-2}$	7.53	−0.22	10,744	$1.685\ 10^{-1}$	9,331	0.14
Ethane	4.384	8,194	$1.693\ 10^{-2}$	8.50	−3.92	9,178	$7.275\ 10^{-2}$	—	—

Meares[21] has suggested that, in the density packed region of the glassy state where the synchronized rotation of chain segments are severely restricted, the diffusing molecule travel by loosening of van der Waals bonds between chain segments and cause compression of the surrounding chains to produce a space of sufficient cross section for the diffusion molecule to pass. Diffusion takes place along a cylindrical cavity of cross section equal to that of the penetrant molecule, $\frac{1}{4}\,d^2$, with the energy required to produce such a cross section. The activation energy of diffusion is related to the volume of the average unit diffusion step by the equation[21]

$$E_D = \tfrac{1}{4}\pi d^2 \lambda N E_c \tag{20}$$

where d is the collision diameter of penetrant gas, λ is the jump distance, N is Avogadro's number, and E_c is the polymer cohesive energy density. Equation (20) suggests that E_D increases linearly with d^2 if the jump distance is constant.

The activation energy of diffusion for n-butane, propane, and ethane versus the square of penetrant diameter is presented in Figure 21. Since Eq. (20) describes the activation energy of diffusion for n-butane, propane, and ethane in ethylcellulose in terms of the polymer and penetrant gas properties, the jump distances λ for a unit diffusion process are calculated from the same equation. The jump distances for n-butane, propane, and ethane are presented in Table IV. A value of 106.1 cal/cm^3 was used for the cohesive energy density of ethylcellulose.[32]

According to the Eyring's transition-state theory of diffusion,[33] the pre-exponential term D_0 in the Arrhenius expression describing the temperature dependence of the diffusivity depends upon λ^2 and ΔS^* as follows,[34]

$$D_0 = e\lambda^2 \frac{kT}{h} \exp\left(\frac{\Delta S^*}{R}\right) \tag{21}$$

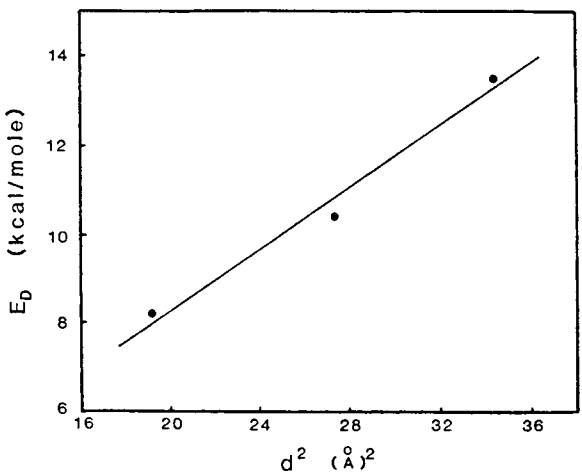

Fig. 21. Correlation of activation energies of diffusion with the square of penetrant molecular diameters.

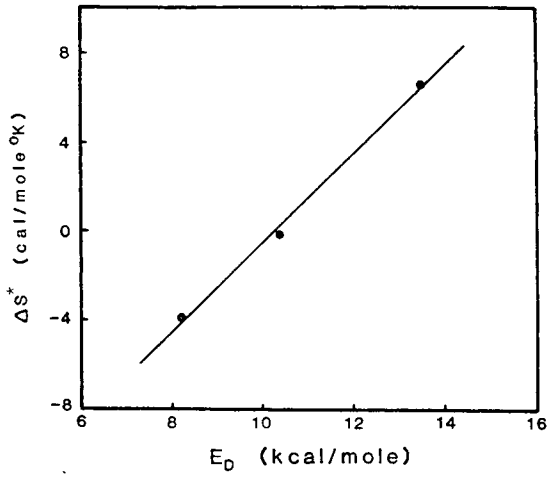

Fig. 22. Correlation of activation energy of diffusion with the entropy of activation.

where $e = 2.72$, k is the Boltzman constant, h is Planck's constant, and ΔS^* is the entropy of activation for diffusion. Using values of λ and D_0 from Table IV, the entropies of activation ΔS^* at 25°C were calculated from eq. (21) and are given in Table IV.

The magnitude of the entropy of activation emphasizes the extent of segmental disturbance by the penetrant gas. The involvement of polymer chains in the unit diffusion process is less for small penetrant molecules and, therefore, both a small activation energy of diffusion and a small S^* is required. As the penetrant size becomes larger, the activation energy increases, as discussed before, and because of more segmental disturbance a larger ΔS^* can be expected. A plot of ΔS^* versus E_D is shown in Figure 22. ΔS^* increases linearly with E_D, as predicted by Barrer's zone theory,[34] and such a linear relationship has been reported by other investigators.[21,24,29]

CONCLUSIONS

This work has shown that the partial immobilization model can accurately describe the transport of n-butane, propane, and ethane in ethylcellulose. The results are consistent with the sorption measurements made on the same system and described by the dual sorption model.[1]

The permeability of the three gases studied is pressure dependent. The decreased pressure dependency of the permeability with increasing temperature can be related to structural changes in the polymer and changes in the sorption and diffusion mechanism. The pressure dependency of the permeabilities is well represented by the partial immobilization model. The strong concentration dependence of the diffusion coefficient in these systems is most likely the result of the low mobility of the Langmuir-mode species.

From an analysis of the temperature dependence of the transport parameters, it was found that the activation energy of diffusion for n-butane, propane, and ethane in ethylcellulose varies as the square of the penetrant diameter.

References

1. E. Casur and T. G. Smith, Paper submitted to *J. Appl. Polym. Sci.* First paper in this series of two.
2. E. Casur, Ph.D. thesis, University of Maryland, College Park, Maryland, 1984.
3. W. R. Vieth, J. M. Howell, and H. H. Hsieh, *J. Membrane Sci.*, **1**, 177 (1976).
4. W. R. Vieth and K. J. Sladek, *J. Colloid Sci.*, **20**, 1014 (1965).
5. W. R. Vieth, C. S. Frangoulis, and J. A. Rionda, *J. Colloid Interface Sci.*, **22**, 454 (1966).
6. W. R. Vieth, P. Tam, and A. S. Michaels, *J. Colloid Interface Sci.*, **22**, 360 (1966).
7. D. R. Paul, *J. Polym. Sci.*, **7**, 1811 (1969).
8. D. R. Paul and D. R. Kemp, *J. Polym. Sci., Symp.*, **41**, 79 (1973).
9. J. H. Petropoulos, *J. Polym. Sci., A-2*, **8**, 1797 (1970).
10. D. R. Paul and W. J. Koros, *J. Polym. Sci., Polym. Phys. Ed.*, **14**, 675 (1976).
11. A. H. Chan, W. J. Koros, and D. R. Paul, *J. Membrane Sci.*, **3**, 117 (1978).
12. W. J. Koros, D. R. Paul, and A. A. Roch, *J. Polym. Sci., Polym. Phys. Ed.*, **14**, 687 (1976).
13. G. S. Huvard, V. T. Stannett, W. J. Koros, and H. B. Hopfenberg, *J. Polym. Sci.*, **6**, 185 (1980).
14. K. S. Yi, Ph.D. thesis, University of Maryland, College Park, Maryland, 1976.
15. P. Y. Hsieh, *J. Appl. Polym. Sci.*, **7**, 1743 (1963).
16. W. J. Koros and D. R. Paul, *J. Polym. Sci., Polym. Phys. Ed.*, **16**, 2171 (1978).
17. W. J. Koros, A. H. Chan, and D. R. Paul, *J. Membrane Sci.*, **2**, 165 (1977).
18. W. J. Koros, D. R. Paul, M. Fujii, H. P. Hopfenberg, and V. T. Stannett, *J. Appl. Polym. Sci.*, **21**, 2899 (1977).
19. A. J. Erb and D. R. Paul, *J. Membrane Sci.*, **8**, 11 (1981).
20. A. C. Newns and G. S. Park, *J. Polym. Sci., C*, **22**, 927 (1969).
21. P. Meres, *J. Amer. Chem. Soc.*, **76**, 3415 (1954).
22. J. O. Hirschfelder, C. F. Curtiss, and R. B. Bird, *Molecular Theory of Gases and Liquids*, Wiley, New York, 1954.
23. P. Masi, D. R. Paul, and J. W. Barlow, *J. Polym. Sci., Polym. Phys. Ed.*, **15**, 20 (1982).
24. S. P. Chen and J. A. D. Edin, *Polym. Eng. Sci.*, **20**, 40 (1980).
25. H. Fujita, *Fortschr. Hochpolym. Forsch.*, **3**, 1 (1961).
26. A. S. Michaels, W. R. Vieth, and J. A. Barrie, *J. Appl Phys.*, **34**, 13 (1963).
27. W. J. Koros and D. R. Paul, *Polym. Eng. Sci.*, **20**, 14 (1980).
28. R. M. Barrer and G. Skirrow, *J. Polym. Sci., C*, **10**, 17 (1965).
29. P. Meares, *Trans. Faraday Soc.*, **53**, 101 (1957).
30. M. Fujii, H. P. Hopfenberg, and V. T. Stannett, *J. Macromol. Sci., Phys.*, **B15**, 421 (1978).
31. H. Yasuda and T. Hirotsu, *J. Appl. Polym. Sci.*, **21**, 105 (1977).
32. J. Brandup and E. H. Immergut, Eds., *Polymer Handbook*, McGraw-Hill, New York, 1975.
32. J. Brandup and E. H. Immergut, Eds., *Polymer Handbook*, McGraw-Hill, New York, 1975.
33. G. Glasstone, K. J. Laidler, and H. Eyring, *The Theory of Rate Processes,* McGraw-Hill, New York, 1941.
34. R. M. Barrer, *Trans. Faraday Soc.*, **38**, 322 (1942).

Received August 21, 1985
Accepted October 21, 1985